Acta Geochim
https://doi.org/10.1007/s11631-024-00683-5

ORIGINAL ARTICLE

# Hydrothermal alteration of the surface volcanic rocks at the Acoculco geothermal field, Mexico: a multi-parametric approach

**America Yosiris García-Soto[1] · Kailasa Pandarinath[1] · E. Santoyo[1] · Eduardo Gonzalez-Partida[2]**

Received: 11 September 2023 / Revised: 20 February 2024 / Accepted: 5 March 2024


**Abstract** The studies on hydrothermal alteration-induced effects in surface and subsurface rocks provide useful information in the characterization and exploitation of a geothermal reservoir. Generally, these studies are based on traditional, and reliable methods like petrography (primary and secondary minerals, and grade of alteration), and geochemistry (mobility of elements, changes in mass and concentration of elements, and fluid inclusions). Recently, apart from these established methods, some methods based on the geochemical (Chemical Index of Alteration, CIA; Weathering Index of Parkar, WIP; Loss on Ignition, LOI; and Sulfur, S) and rock magnetic properties (magnetic susceptibility, χlf; and percentage frequency-dependent susceptibility, χfd%) are also being applied in the identification of whether a rock is an altered or a fresh one. The Acoculco Geothermal Field (AGF), Mexico, is characterized by high temperature and very low permeability, and it is considered a promissory Enhanced Geothermal System. The following changes are observed in the rocks as a result of an increase in hydrothermal alteration: (1) an increase in CIA, LOI, and S values, and a decrease in WIP; (2) an increase in quartz and quartz polymorph minerals (silicification), and clay minerals (argillization); and (3) decrease in χlf values. At AGF, the most altered surface acid rocks are characterized by entirely quartz and its polymorphs, and clay minerals. The present study also indicates the applicability of the binary plots of major elements (felsic vs mafic component) and rock magnetic parameters (χlf vs. χfd%). The rock with χfd% value of 2–10 and χlf value $< 0.5 \times 10^{-6}$ $m^3$ $kg^{-1}$ indicate the presence of single domain and stable single domain grains, which in turn suggests that it is an altered rock. These methods are simple to apply, rapid, reliable, and have the potential to become effective tools for the identification of hydrothermally altered rocks during the initial stage of geothermal exploration.

**Keywords** Geothermal fields · Hydrothermal alteration · Surface rocks · Magnetic susceptibility · Alteration indices

## 1 Introduction

In geothermal areas, hydrothermal fluids produce physicochemical changes in the rocks through which they circulate (Pirajno 2009). When the thermal fluids react with rocks, they initiate chemical reactions and alter primary minerals through processes of dissolution, ion exchange, replacement, precipitation, and (or) recrystallization (Berger 1998). Temperature, pressure, the chemical composition of the rocks and fluid, and the water–rock ratio are some of the physicochemical parameters that control the type and extent of hydrothermal alteration (Stefánsson and Kleine 2017). Hydrothermal alteration is a common process in geothermal systems and can significantly change the physicochemical properties of rocks (Weyd et al. 2022). Identifying the distribution of hydrothermally altered rocks and understanding the prevailing hydrothermal alteration processes provide information about the size of a geothermal system and the thermal

**Supplementary Information** The online version contains supplementary material available at https://doi.org/10.1007/s11631-024-00683-5.

✉ Kailasa Pandarinath
pk@ier.unam.mx

[1] Instituto de Energías Renovables, Universidad Nacional Autónoma de México, Priv. Xochicalco s/no., Col. Centro, Apartado Postal 34, 62580 Temixco, Morelos, Mexico

[2] Centro de Geociencias, UNAM, Apartado Postal 1-742, 76001 Querétaro, Querétaro, Mexico

Published online: 08 April 2024

conditions prevailing in the region. The classification of mineral alteration assemblages provides information on the mechanisms and the conditions under which the alteration occurred, and this information can be used in the characterization and exploitation of a reservoir (Brown and Ellis 1970; Brown 1978; Lagat 2009). Generally, hydrothermal alteration at depth is studied based on traditional and well-established methods like petrography, geochemical, mineralogical, and fluid inclusions (Lagat 2009; Franco 2016; Pereira et al. 2022). These methods are expensive, involve laborious sample preparation methodology, and need experts to carry out these laboratory works. This suggests a need for other reliable methods that are less expensive and easy to operate.

The rock magnetic parameters along with various parametric ratios obtained from them are applied in the identification of the variations in the magnetic material concentration and grain sizes about erosion, soil formation (Maher and Taylor 1988), sediment source (Walling et al. 1979; Geiss et al. 2008; Hatfield and Maher 2009), pollution (Hoffmann et al. 1999), diagenesis (Roberts and Turner 1993; Larrasoaña et al. 2007) and paleomonsoon and paleoclimate studies (Maher et al. 1994, 2002). There are some studies on hydrothermally induced changes in magnetic properties of oxidized A-type granites (Nédélec et al. 2015) and Archean granitic plutons (Lapointe et al. 1986), and identification and mapping of hydrothermal zones during exploration and operation of porphyry Cu deposits in Northern Chile (Riveros et al. 2014). However, the studies on the applicability of rock magnetic parameters in the identification of hydrothermally altered volcanic rocks and zones of hydrothermal alteration in perspective of geothermal fields are very limited (Krafla geothermal field, Iceland, Oliva-Urcia et al. 2011; Los Azufres Geothermal Field, LAGF, Mexico, Pandarinath et al. 2014, 2019). The main objective of the present work is to carry out a multi-parametric approach to retrieve the hydrothermal alteration record for the surface volcanic rocks of AGF, Mexico. For this purpose, we have applied the geochemical (binary diagram of felsic and mafic components of major elements oxides; Chemical Alteration Indices, CIA; Weathering Index of Parkar, WIP; Loss on Ignition, LOI; Sulfur-content, S content), mineralogical methods (primary and hydrothermal minerals), and the rock magnetic parameters ($\chi$lf and $\chi$fd%) in identification of altered rocks. Additionally, the present work may also serve as an additional validation of the applicability of the rock magnetic methods. As of now, these parameters are successfully applied for liquid dominate LAGF, and super-hot vapor dominate LHGF, and the present work is proposed to carry out with the surface rocks of AGF, a hot dry rock (enhanced) geothermal system.

## 2 Acoculco geothermal field (AGF): the study area

Acoculco Caldera is located in the eastern part of the Trans-Mexican Volcanic Belt and the northern part of the Puebla state of Mexico. The study area includes a geothermal prospective area, characterized by high temperature, and very low permeability, and has been considered a promissory site for future enhanced (engineered) geothermal system (EGS; López-Hernández et al. 2009; Sánchez-Córdova et al. 2020), which is also known as a hot dry rock (HDR) system. López-Hernández et al. (2009) have reported that the Acoculco Caldera is 18 km in diameter and the volcanic rocks associated with Tulancingo-Acoculco Caldera Complex have been the site of three distinct hydrothermal events: (1) The emplacement of Mid-Tertiary granitic intrusions that metamorphosed the sedimentary rocks; (2) The formation of the Tulancingo and Acoculco Calderas; and (3) A possible third hydrothermal event may be associated with the recent magmatic activity within the Acoculco Caldera. They also reported some volcanic rocks such as rhyolites, dacites, basalts and rhyolitic ignimbrites in the Acoculco caldera and these formations were intercalated with Apan and Tecomulco basalts and basaltic andesites in the surroundings of the Tulanciongo-Acoculco caldera. However, recent studies (Avellán et al. 2018), suggest the existence of only an asymmetric caldera ($18 \times 16$ km) with an intra-caldera ignimbrite, and uplifted sediments. They have not found evidence of a larger caldera structure (Tulancingo caldera). Avellán et al. (2018, 2019) and Sosa-Ceballos et al. (2018) presented geologic maps with 40 lithostratigraphic units of the caldera and describe its geochemical evolution, respectively, lumped into five successions to caldera formation: (1) Extra-caldera volcanism (ca. 0.90–$<$0.06 Ma), (2) Late post-caldera volcanism (ca. 2.0–1.0 Ma), (3) Early post-caldera volcanism (ca. 2.6–2.2 Ma), (4) Caldera-forming eruption (ca. 2.7 Ma) and (5) Pre-caldera volcanism (ca. 2.4–0.19 Ma) and one Miocene unit that represents an early stage of the Trans-Mexican Volcanic Belt (TMVB). The three major geothermal fields (LAGF, LHGF, and AGF) are situated within the Trans-Mexican Volcanic Belt (TMVB), a continental volcanic arc. LHGF and AGF are in the eastern part of the TMVB, whereas LAGF is in the center of the TMVB.

Due to the presence of surface manifestations and extensive surface hydrothermal alteration, cold-acid springs, and constant gas discharges, two exploratory wells were drilled in the area: the well EAC-1 was drilled to a depth of 1810 m in 1995, and the well EAC-2 was drilled to a depth of 1900 m in 2008 (Viggiano-Guerra et al. 2011). There are some studies on mineral alteration and fluid inclusion of drill cuttings and core samples (López-Hernández et al. 2009; Canet et al. 2010; González-Partida et al. 2022). These studies have shown that the hydrothermal system is not very active at present. However, surface gas emissions,

the high temperatures measured in well EAC-1, and the hot springs at Chignahuapan suggest that there is a hidden active hydrothermal system in the study area. The intense secondary mineral deposition in the pyroclastic deposits created a very effective caprock that prevents the ascent of high-temperature fluids to the surface. Among the identified mineral assemblages are buddingtonite and smectite in the caldera sequence, and calcite marble and granitic rocks. Canet et al. (2010) have reported two major zones of hydrothermal alteration at the Acoculco Caldera, the shallower zone contained ammonium illite and the deeper zone consists of epidote-calcite-chlorite mineral assemblages. Recently, Sánchez-Córdova et al. (2020) have reported the water–rock interactions, particularly, paragenesis and elemental mass balance in the Acoculco geothermal system. Detailed surface rock studies were conducted in an area where two exploratory wells have been drilled. Mineralogical studies have identified minerals such as kaolinitic clays, chalcedonic quartz, and pyrite (Viggiano-Guerra et al. 2011). Canet et al. (2015) have suggested that the silicic alteration is the most widespread affecting the surface rocks and indicate three prospective areas, Alcaparrosa, Los Azufres, and Las Minas, by the cooccurrence of acid-sulfate alteration, buddingtonite and ammonium anomalies.

## 3 Collection of rock samples and analytical methods

64 rock samples from the surface region of Acoculco caldera were selected representing the entire study area (Fig. 1). These samples were contributed by Dr. Eduardo Gonzalez-Partida, one of the co-authors of this article, and his group. The methodology followed for various laboratory analyses and calculations carried out on the rock samples is mentioned below.

The mineralogical composition of the rock samples is obtained by the X-ray diffractometer (XRD machine; Rigaku model DMAX 2200) at the Instituto de Energies Renovables (UNAM). The diffractometer is equipped with Cu Kα

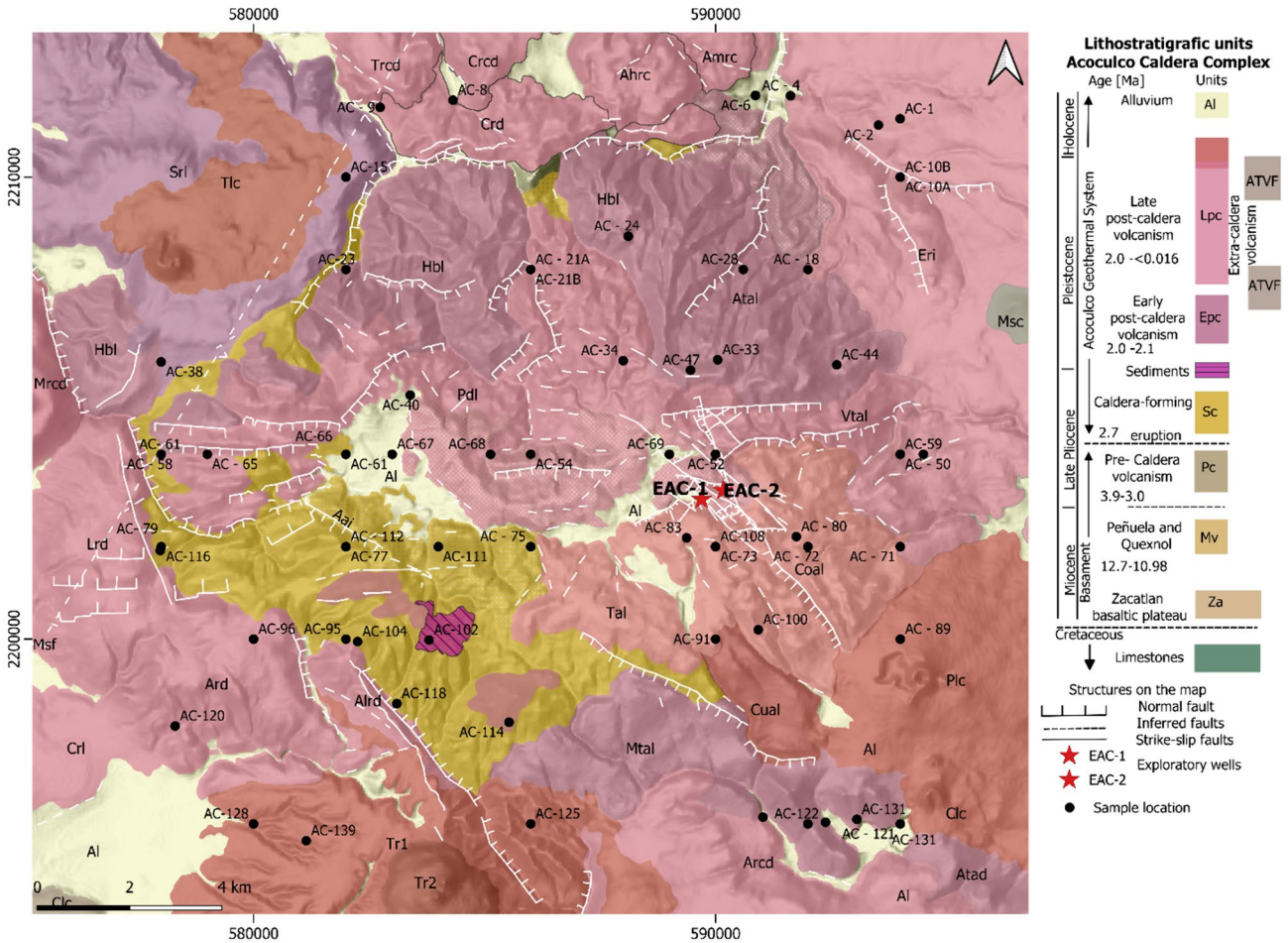


**Fig. 1** Geological map along with the locations of the surface rocks at the Acoculco Geothermal Field, Mexico. This map is taken from Avellán et al. (2020) and modified with the tectonic features reported from Bolós et al. (2022)

radiation (λ = 1.54 Å), a secondary graphite monochromator, and a scintillation detector. The rock samples were finely powdered and filled with the sample holders. To obtain all the minerals in the samples, they were scanned with 40 kV and 40 mA, from two-theta of 0°–60°. The JADE 6.5 software, which is integrated with the XRD machine, is used for the identification of the minerals. The rocks with the dominant presence of primary minerals are considered fresh rocks, whereas the secondary minerals predominate in the altered rocks.

Geochemical analyses of 64 rock samples are carried out at the Activation Laboratories Ltd., Ontario, Canada (Actlabs). Major and trace elements were determined by ICP-OES (inductively coupled plasma-optical emission spectrometry) and ICP-Mass spectrometry (MS). The lithium tetraborate fusion technique was employed for sample dissolution. All major element oxides and some trace elements were analyzed by ICP-OES. LOI is measured by FUS-ICP with the obtained All REEs and some trace elements were determined by INAA (instrumental neutron activation analysis). The surface rock samples from a geothermal area seldom occur as fresh rock, instead, they will be intensive to least altered. Hence, the surface rock samples collected from the surface region of AGF cannot be classified by the TAS diagram method, as this method is meant for the classification of fresh rocks. Due to this, we have applied the classification method for altered rocks proposed by Verma et al. (2017) and applied the computer program (MagClaMSys_ilr). This method classifies the igneous rocks in terms of four magma types: ultrabasic, basic, intermediate, and acid. This multidimensional classification scheme is based on isometric log-ratio (ilr) transformation and probability estimates and showed correct classification with high percent success rates.

The binary diagram with the total concentrations of CaO, $K_2O$, and $Na_2O$ (represented mainly by felsic mineral component; feldspars) on the X-axis and $Fe_2O_3^T$, MnO, and MgO (represented mainly by mafic minerals component; pyroxenes, amphiboles etc.) on the Y-axis may be used to differentiate fresh and altered rocks (Fig. 2). The rock samples located near to the origin of the plot may be considered as altered to intensively altered rocks, whereas those plotted away from the origin of the plot are relatively fresh (least to less altered). The lower values of both the axes (near the origin) may be interpreted as the high intensity of alteration (Fig. 2a–c) and as the values of the axes increase (moves away from the origin), the intensity of alteration decreases.

Pandarinath (2022) has carried out the validation and the applicability of a total of 47 alteration indices in distinguishing the fresh and altered rocks of six Mexican Geothermal Fields. He has also identified 15 best-performer indices for the six Mexican geothermal fields. In the present work, two reliable alteration indices (CIA, Nesbitt and Young 1982;

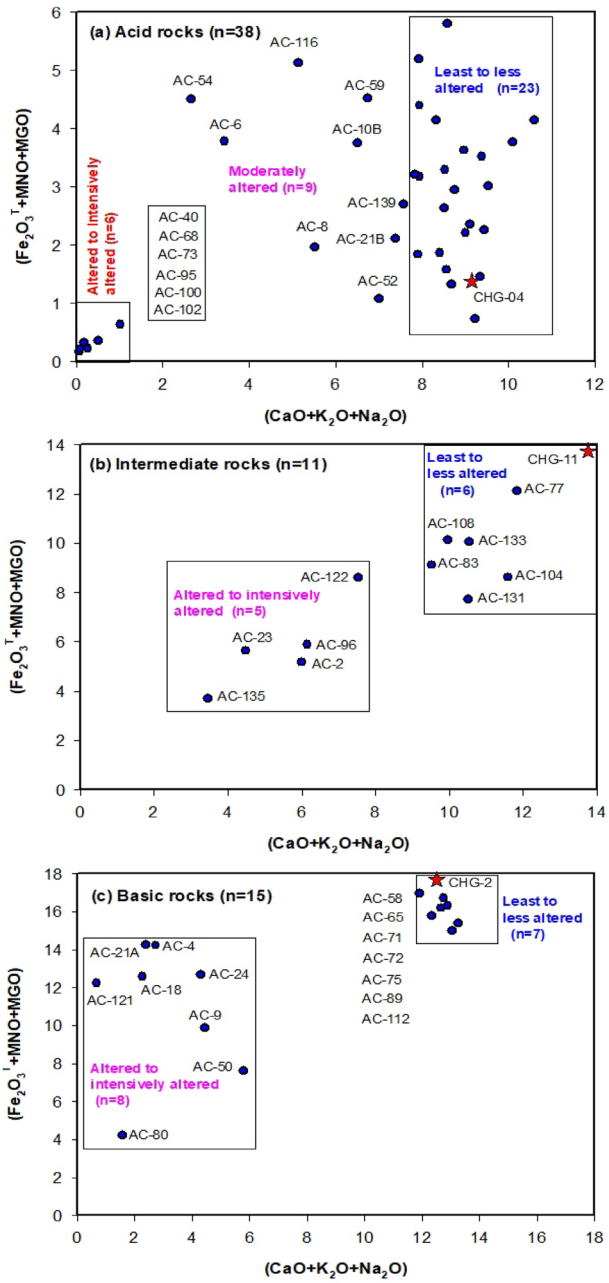


**Fig. 2** The binary diagram of felsic ($CaO + K_2O + Na_2O$) versus mafic component ($Fe_2O_3^T + MnO + MgO$ for each type of rocks; **a**, **b**, and **c** represent the acidic, intermediate, and basic rocks, respectively

and WIP, Parker 1970) were applied to identify whether a rock is fresh or has undergone alteration. CIA presents the degree of chemical alteration of rocks, interpreted as a measure of the change of feldspar minerals to clay minerals, and its values increase in parallel with the increase in clay minerals in the rock (Nesbitt and Young 1982). Pandarinath (2023) has reported a good performance by these two indices in the identification of least to less and altered to intensively altered and are categorized CIA of Nesbitt

and Young (1982) and WIP of Parker (1970) in the first and fifth places, respectively in a total of 47 chemical indices. For fresh rocks, CIA values are < 60% whereas for altered rocks its values are > 60% (Nesbitt and Young 1982, 1984; McLennan 1993). Similarly, for fresh rocks, WIP values are > 60% whereas for altered rocks their values are < 60% (Parker 1970).

The Eq. (1), for calculating CIA is mentioned below.

$$\mathrm{CIA} = \left( \frac{\mathrm{Al_2O_3}}{\mathrm{Al_2O_3} + \mathrm{CaO} + \mathrm{Na_2O} + \mathrm{K_2O}} \right) \times 100 \quad (1)$$

In this equation, the concentrations of the major element oxides are in molecular proportion. Molecular proportions of major element oxides were calculated by dividing the weight percent of major element oxides by their molecular weight. The CaO content should represent that incorporated in the silicate fraction (CaO*) of the rocks.

Parker (1970) proposed the Index of weathering for silicate rocks, where hydrolysis is the main agent of silicate weathering. The hydrolysis process results in the physical disaggregation of rocks and the removal of mobile elements. In the case of WIP, its values decrease with the increasing grade of alteration (Parker 1970; Takahashi and Shimaoka 2012). For fresh rocks, WIP values are > 60% whereas for altered rocks are < 60%.

$$\mathrm{WIP} = \left( \frac{(\mathrm{Na})_a}{0.35} + \frac{(\mathrm{Mg})_a}{0.9} + \frac{(\mathrm{K})_a}{0.25} + \frac{(\mathrm{Ca})_a}{0.7} \right) \times 100 \quad (2)$$

where $(\mathrm{x})_a$ represents the atomic proportion (atomic percentage divided by atomic weight) of the element.

Magnetic susceptibility (χlf) is measured based on the method suggested by Dearing (1999). Small fragments of rocks are packaged in non-magnetic cylindrical plastic bottles of 10 $cm^3$. χlf *is* measured at low (0.47 kHz; $\chi_{lf}$) and high (4.7 kHz; $\chi_{hf}$) frequencies with a Bartington Susceptibility Meter (Model MS2B) and a dual frequency sensor. From these measurements, the mass-specific magnetic susceptibility (hereafter it is referred to as χlf) is obtained and the percentage of frequency dependent magnetic susceptibility ($\chi_{fd}\%$) was calculated, using the equation (Eq. 3) proposed by Dearing (1999).

$$\chi_{fd(\%)} = \frac{(\chi_{lf} - \chi_{hf}) \times 100}{\chi_{lf}} \quad (3)$$

## 4 Results

64 rock samples collected from the surface of AGF are used in the present work. The locations of the rock samples, rock type, and other details are shown in Supplementary Table S1. To avoid the lithological influence in all the processes, we present the results and interpretations separately for each rock type: acid (38 samples), intermediate (11 samples), and basic (15 samples). It is rare to find completely fresh surface rocks in geothermal areas as they are subjected to less or more alteration by existing processes in these areas. Therefore, in this article, we are reporting as least to less altered and altered to intensively altered rocks instead of fresh and altered rocks, respectively. Table 1 presents the different methods applied in the identification of hydrothermal alteration and the average number of rocks identified as least to less altered and altered to intensively altered.

**Table 1** Details of the methods applied in the identification of hydrothermal alteration and the average number of rocks identified as least to less altered and altered to intensively altered in the surface rocks of Acoculco Geothermal Field, Mexico

| Alteration type | Magma type | Binary plot (Fel vs. Maf) (Fig. 2a–c) | CIA (Fig. 3a–c) | WIP (Fig. 3d–f) | LOI (wt%) (Fig. 4a–d) | Sulfur (ppm) (Fig. 5a–c) | Xlf (Fig. 6a–c) | χlf versus χfd% (Fig. 7a–c) |
|---|---|---|---|---|---|---|---|---|
| *(a) Acid rocks* | | | | | | | | |
| Alt-Int alt | Acid | 15 | 17 | 14 | 21 | 14 | 19 | 19 |
| Least-Less alt | Acid | 23 | 21 | 24 | 17 | 24 | 19 | 19 |
| *(b) Intermediate rocks* | | | | | | | | |
| Alt-Int alt | Intermediate | 05 | 05 | 05 | 06 | 03 | 02 | 02 |
| Least-Less alt | Intermediate | 06 | 06 | 06 | 05 | 08 | 09 | 09 |
| *(c) Basic rocks* | | | | | | | | |
| Alt-Int alt | Basic | 08 | 08 | 08 | 08 | 08 | 03 | 07 |
| Least-Less alt | Basic | 07 | 07 | 07 | 07 | 07 | 12 | 08 |

CIA: chemical index of alteration (Nesbitt and Young 1982); WIP: weathering index of Parker (Parker 1970): LOI: loss-on-ignition: χlf: magnetic susceptibility (measured at low frequency; χfd%: frequency dependent susceptibility (%). Alt-Int alt: altered to intensively altered; least-less alt: least to less altered: Fel: Felsic: Naf; Mafic

### 4.1 Mineral data

The XRD technique was used to analyze the mineral composition of all the rock samples. The primary minerals identified in the least to less altered rocks are plagioclase, orthoclase, microcline, sanidine, phlogopite, and quartz. In contrast, the intensively altered rocks contain the following secondary minerals: quartz, quartz polymorphs (cristobalite, tridymite, and opal), alunite, greigite, hematite, and clay minerals halloysite, kaolinite, and dickite. Almost all the rocks of the present study contained quartz and quartz polymorphs minerals, with varying contents. The dominant contents of cristobalite, quartz, and tridymite are observed in 18, 8, and 5 out of the total 64 rocks, respectively. This suggests that silicification is the dominant alteration process followed by rare argillization at AGF (Supplementary Table S2).

### 4.2 Geochemical data

#### *4.2.1 Binary diagram of felsic and mafic component*

Plotting of 38 acid rocks of the present study indicated their distribution in three groups, The first group consists of six acid rocks (AC-40, AC-68, AC-73, AC-95, AC-100, and AC-102; Fig. 2a) that are very nearer to the origin (or almost at the origin) of the diagram. The mineral composition of these rocks indicates that five rocks (AC-40, AC-68, AC-73, AC-95, AC-100) contain only quartz and quartz polymorphs (cristobalite, and tridymite; Supplementary Table S2), and the sixth one (AC-102) contains only clay minerals (kaolinite and dickite; Supplementary Table S2). This suggests that these six rocks have undergone an intensive alteration, with the complete dissolution of both felsic and mafic primary minerals and intense silicification (precipitation of quartz) in five rocks and argillization in the sixth rock. The second group with nine acidic rock samples (AC-54, AC-116, AC-6, AC-59, AC-10B, AC-139, AC-8, AC-21B, and AC-52) is located between group 1 (zone of "altered to intensively altered") and the third group of rocks (n = 23) located farthest from the origin (zone of "least to less altered") indicating that rocks from the group 2 are "less to moderately altered" (Fig. 2a).

Plotting of 11 intermediate rocks in the binary diagram (Fig. 2b) resulted in two groups. Six rock samples (AC-77, AC-108, AC-133, AC-83, AC-104, and AC-131) were plotted away from the origin of the diagram, indicating that these rocks are "least to less altered". To check the reliability of this conclusion, we have plotted a fresh trachyandesite rock (intermediate rock, CHG-11, shown as a star symbol in Fig. 2b) from the surface of AGF (Verma 2001), which also plotted within the group of six rocks (Fig. 2b). This confirms that these 6 intermediates (andesite) rocks are least to less altered. The remaining five intermediate rocks (AC-122, AC-23, AC-96, AC-2, and AC-135) were plotted as a group towards the origin of the plot, indicating that these five rock samples are "altered to intensively altered" (Fig. 2b).

Plotting of 15 basic rocks in the binary diagram (Fig. 2c) has resulted in two groups. Seven rocks are "least to less altered" and eight rock samples are "altered to intensively altered" (Fig. 2c). To check the reliability of this conclusion, we have plotted a fresh basalt rock (basic rock, CHG-2, shown as a star symbol in Fig. 2c) from the surface of AGF (Verma 2001), which also plotted within the group of seven rocks (Fig. 2c). This confirms that these seven basic (basalt) rocks are least to less altered. The remaining eight rocks were plotted as a group towards the origin of the plot, indicating that these eight rock samples are "least to less altered" (Fig. 2c).

#### *4.2.2 Chemical alteration indices*

Chemical alteration indices are multi-component ratios of litho-geochemical data, which are used in estimating the alteration intensity of the rocks (Gifkins et al. 2005). Application of these indices is based on assumptions that the concentration of chemical elements is controlled solely by the degree of alteration.

CIA values of 38 acid rocks vary between 49.9 and 94.2, with 17 altered acid rocks (CIA > 60) and 21 fresh acid rocks (CIA < 60, Fig. 3a). CIA values of 11 intermediate rocks vary between 46.6 and 81.5, with six intermediate rocks being fresh (CIA < 60; Fig. 3b) and the remaining five intermediate rocks are being altered (CIA > 60; Fig. 3b). Finally, CIA values of 15 basic rocks vary between 42.8 and 96.1, with seven basic rocks are being fresh (CIA < 60) and the remaining eight basic rocks are being altered (CIA > 60; Fig. 3c).

The application of the Weathering Index of Parker (WIP) to 38 acidic rocks leads to a value range of 0.4 and 84.3. WIP values for 14 acid rocks indicated that these rocks are altered (WIP < 60; Fig. 3d) and the remaining 24 acid rocks are fresh having the WIP values varying between 60.1 and 84.3 (> 60; Fig. 3d). WIP values for 11 intermediate rocks varies between 25.5 and 77.1 with five intermediate rocks are altered (WIP < 60; varying between 25.5 and 57.9; Fig. 3e) and the remaining six intermediate rocks are fresh having the WIP values varying between 69.6 and 77.1 (> 60; Fig. 3e). Finally, WIP values for 15 basic rocks varies between 4.7 and 80.0 with seven rocks are fresh (WIP > 60; varying between 72.3 and 80.0; Fig. 3f) and the remaining eight basic rocks are altered having the WIP values varying between 4.7 and 40.4 (< 60; Fig. 3f).

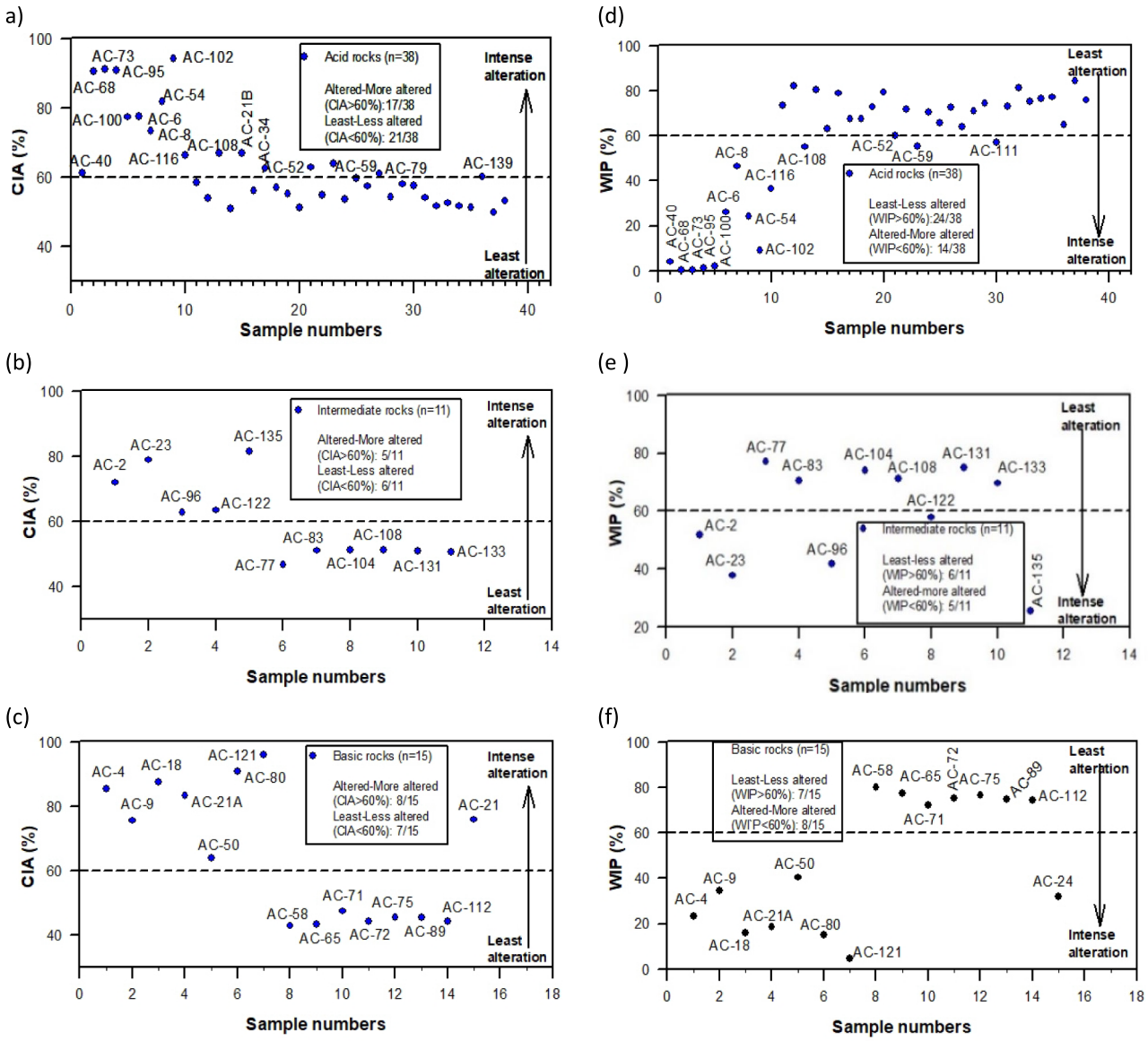


**Fig. 3** The binary diagrams of sample numbers versus CIA (**a**, **b**, and **c**) and sample numbers versus WIP (**d**, **e**, and **f**) for each rock types

### *4.2.3 Loss-on-ignition*

Loss-on-ignition (LOI) is defined as the water content of rocks (Johnson and Maxwell 1981). However, it has been considered unreliable that LOI represents only the $H_2O^+$ content of rocks because there are volatile components ($CO_2$, F, Cl, S, etc.) and oxidizable Fe in rocks other than water, which also contribute along with $H_2O^+$ to the LOI (Lechler and Desilets 1987). Suoeka et al. (1985) have reported that the higher the LOI values, the more the intensity of alteration. The total volatile content of the rock is determined by ignition at 1000 °C for an hour and the resulting weight loss is expressed as LOI, which is useful as an indicator of alteration of volcanic rocks resulting from hydration or calcitization of mafic minerals. In volcanic rocks, a higher content of $H_2O^+$ results due to the hydration and clay minerals formation during alteration. Intense alteration conditions favor the formation of hydrothermal clay minerals (kaolinite, halloysite, limonite, goethite, etc.). This, in turn, increases LOI content in the rocks because the clay minerals contain a significant amount of $H_2O^+$ in their crystals. The content of LOI also varies by the type of the rocks and the type and the content of clays (Jayaverdena and Izawa 1994). Altered rocks have relatively high LOI compared to their host rocks (MacKenzie and Craw 2007). Considering the LOI values of 2 wt% (Le Bas et al. 1986) or 2.5 wt% (Matsuno et al. 2022) as a limit to differentiate the fresh and altered rocks of the present study, only a few rocks are identified as fresh,

which is not comparable to other used methods, as the number of samples is significantly different. However, when LOI value of 3 wt% (an arbitrarily selected value) is considered as a limit (dotted horizontal line; Fig. 4) the number of rocks differentiated as least to less and altered to intensively altered rocks are comparable to those obtained by CIA, and WIP methods. Apart from this, three USGS standard reference materials (which are generally considered fresh rocks)

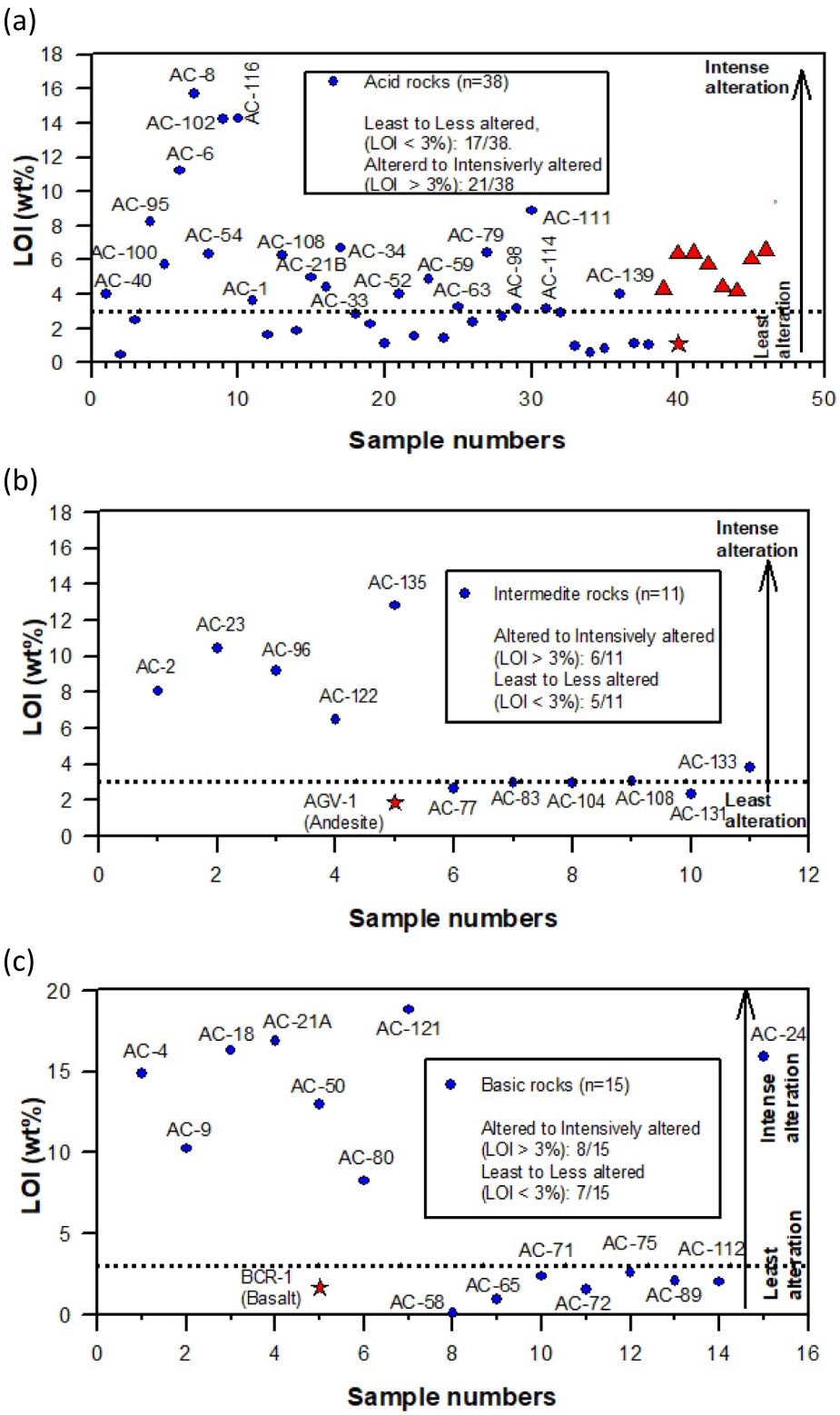


**Fig. 4** The binary diagrams of sample numbers versus LOI (**a**, **b**, and **c**) for each rock types. Triangles filled with red color are altered rhyolite rocks from Hikov et al. (2002). Star filled with red color is a fresh rock (USGS standard RGM-1; rhyolite rock)

RGM-1 (rhyolite/felsic rock), AGV-1 (andesite/intermediate rock), and BCR-1 (basalt/mafic rock), hydrothermally altered rock samples of Hikov (2002), and the rocks of the present study are plotted in the figures (Fig. 4a–c). 17 acid rocks of the present study are located along with RGM-1 (star symbol filled with red) in Fig. 4a, and five intermediate rocks are located with AGV-1 (star symbol filled with blue) in Fig. 4b, and six of the basic rocks are located with the fresh basalt BCR-1 (star symbol filled with green) in Fig. 4c.

In the present work, the LOI content of 38 acid rocks varies between 0.45 and 15.69 wt%. Considering the LOI value of > 3 wt% for altered rocks (Fig. 4b), 21 out of 38 rocks are altered and the remaining 17 are least to less altered. All eight hydrothermally altered rocks from Hikov (2002) are correctly plotted above the dotted horizontal line, whereas the fresh USGS standard reference material RGM-1 (rhyolite) is appropriately located below the line (Fig. 4b). This shows the consistency in the identification of acid rocks.

LOI content of 11 intermediate rocks of this work varies between 0.38 and 12.81 wt%. LOI values of six intermediate rocks are of > 3 wt% (intensively altered), whereas the remaining five intermediate rocks are of < 3 wt% (Fig. 4c). The fresh USGS standard reference material AGV-1 (andesite) is appropriately located below the line (Fig. 4c). This shows consistency in the identification of intermediate rocks.

LOI content of 15 basic rocks of the present work varies between 0.07 and 18.82 wt%. Eleven out of 15 basic rocks are plotted in the zone of altered to intensively altered rocks (Fig. 4d). In the case when LOI values of > 3 wt%, 8 out of 15 basic rocks are located in the zone of intense alteration, whereas the remaining seven basic rocks are located in the zone of least alteration when LOI values are < 3 wt% (Fig. 4d).

#### *4.2.4 Sulfur content*

Sulfur is present in the rocks as sulfides, sulfates, or a mixture of the two. Alkaline rocks (Na and K enriched) usually have higher sulfur contents. Arikawa (1987) has determined the sulfur content in 140 samples of Japanese volcanic rocks and reported widely scattered values of 10–5390 ppm, with a mean value of 116 ppm. Sulfur content in intermediate igneous rocks (andesitic) rocks varies from 1000 to 6700 ppm (Anderson 1974), while Moore and Fabbi (1971) have reported the juvenile sulfur average content of 800 ± 150 ppm for basalt magma (freshest). Notwithstanding, extremely low values are reported in the literature for volcanic rocks. Rhyolites have generally low values of S content (< 0.01 wt%; 100 ppm) and 300 ppm of S content (an average) has been established for several igneous rocks, including basalts, by Turekian and Wedepohl (1961). S value of 62 ppm is reported for the average composition of the upper continental crust by Rudnick and Gao (2003). Close to our study area AGF, in LAGF, Verma et al (2018) have reported S content values varying from 80 to 28,300 ppm for surface rhyolite rocks. They defined the intensity of alteration based on S content in the rocks with < 150 ppm are least to less altered, while the rocks with > 150 ppm are considered as altered to intensively altered rocks. According to them, the mineralogical data sustained the conclusions based on S content. The S values in the rhyolitic rocks of the present study are similar to an average S value (80–830 ppm) reported for rhyolitic rocks by Naldrett et al. (1978). Considering all these cases, S value of 80 ppm is considered as a possible limit to differentiate the least to less altered from the altered to intensively altered rocks. S content in three types of volcanic rocks from the present study area is presented as follows:

S content of 38 acid rocks of this work show wide scattering varies between 10 and 32,900 ppm. There are 13 out of 38 acid rocks located in the zone of altered acid rocks (S > 80 ppm; Fig. 5a), where an S value of 80 ppm is considered as the limit to differentiate the least to less altered from the altered to intensively altered rocks (Fig. 5a).

S content of 11 intermediate rocks of this study area varies between 20 and 310 ppm. S value of 80 ppm is considered as the limit between altered and fresh rocks (Fig. 5b). Eight out of 11 intermediate rocks are plotted in the zone of least to less altered (< 80 ppm), whereas the remaining three intermediate rocks (AC-108, AC-135, and AC-96) are located in the zone of more alteration (S values are > 80 ppm; Fig. 5b).

S content of 15 basic rocks of the present work varies between 20 and 27,000 ppm. 8 out of 15 basic rocks are plotted in the zone of altered to intensively altered rocks, whereas the remaining seven basic rocks are plotted in the zone of least to less altered (Fig. 5c).

### 4.3 Magnetic parameters

The magnetic susceptibility ($\chi$lf) of a rock sample is the sum of the contributions of all rock-forming minerals, and its value depends on the concentration of these magnetic minerals. In the present study area of AGF, $\chi$lf values for the surface acid rocks (n = 38), intermediate rocks (n = 11) and basic rocks (n = 15) vary between 0.01 and $4.9 \times 10^{-6}$ $m^3$ $kg^{-1}$, 0.4 and $12.8 \times 10^{-6}$ $m^3$ $kg^{-1}$, and 0.03 and $13.9 \times 10^{-6}$ $m^3$ $kg^{-1}$, respectively (Fig. 6a–c). This shows that, in the surface rocks of AGF, $\chi$lf values of acid rocks < intermediate rocks < basic rocks. Based on the $\chi$lf values reported for several volcanic rocks in the literature, $\chi$lf value of $\leq 1 \times 10^{-6}$ $m^3$ $kg^{-1}$ is considered a limit in this study for altered to intensively altered rocks. Nineteen out of 38 acid rocks (AC-1, AC-6, AC-8, AC-15, AC-21B, AC-40, AC-52, AC-67, AC-68, AC-95, AC-98,

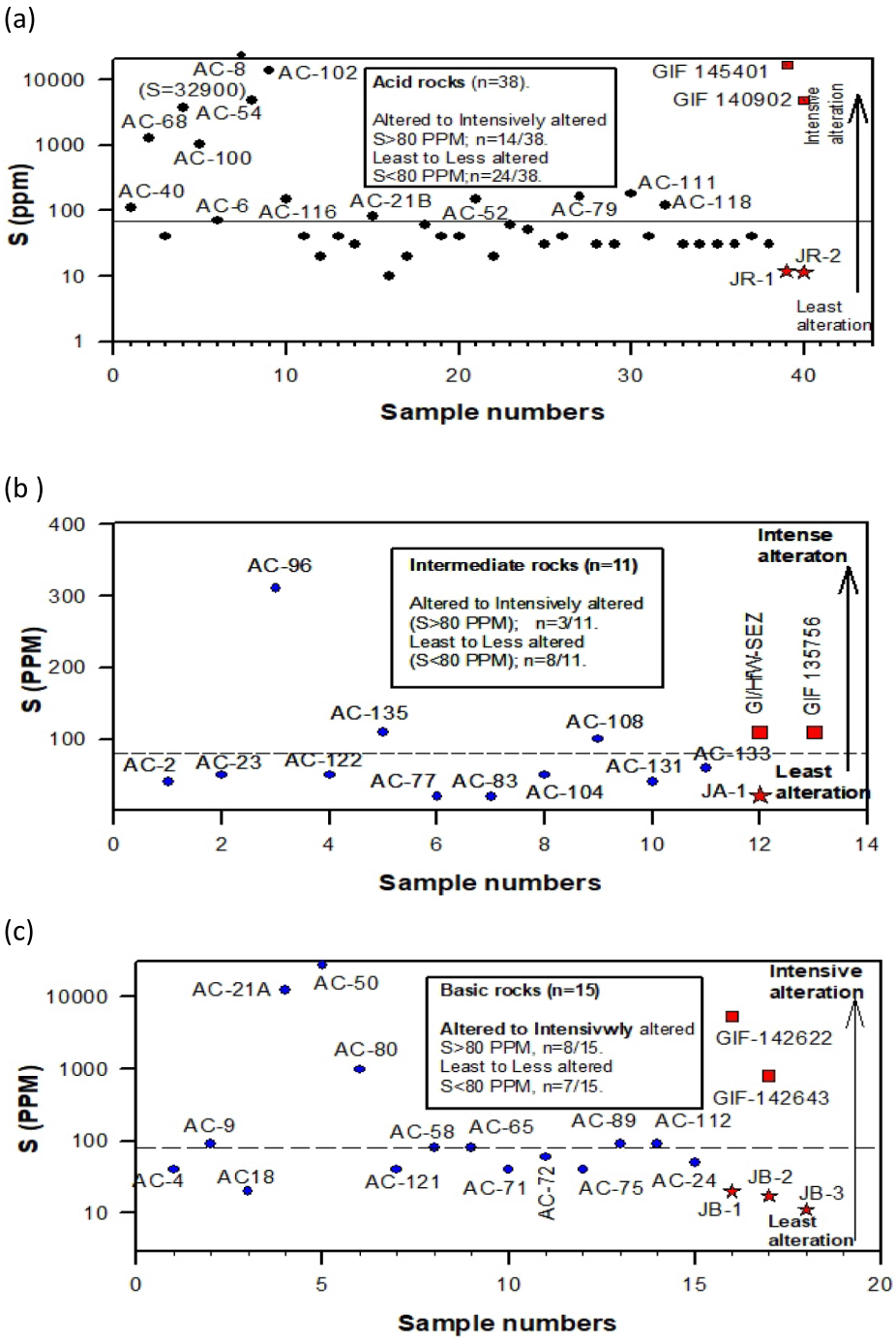


**Fig. 5** The binary diagrams of sample numbers versus sulfur (S) for each rock types (**a**, **b**, and **c**). Data points indicated by squares filled with red color are intensively altered rhyolite (**a**), andesite (**b**) rocks from Gifkins et al. (2005), whereas stars filled with red color are standard refence rhyolite rocks (fresh rocks, JR-1 and JR-2) of Geological Survey of Japan (GSI) is a fresh rock (USGS standard RGM-1; rhyolite rock)

AC-100, AC-102, AC-111, AC-114, AC-116, AC-125, AC-128, and AC-139) have $\chi$lf values $\leq 1.0 \times 10^{-6}$ m$^3$ kg$^{-1}$ (Fig. 6a) indicating that these 19 acid rocks have undergone an intensive alteration, whereas the remaining 19 acid rocks (AC-10A, AC-10B, AC-28, AC-33, AC-34, AC-38, AC-44, AC-47, AC-54, AC-56, AC-59, AC-61, AC-63, AC-69, AC-73, AC-79, AC-91, AC-118, and AC-120) have $\chi$lf values $> 1.0 \times 10^{-6}$ m$^3$ kg$^{-1}$ (varies between 2 and $5 \times 10^{-6}$ m$^3$ kg$^{-1}$), thus considered as least to less altered rocks (Fig. 6a). Among the intermediate rocks, two rocks, AC-96, and AC-135, are characterized by $\leq 1 \times 10^{-6}$ m$^3$ kg$^{-1}$ and considered as altered to intensively altered, whereas the remaining nine rocks represent the least to less altered (Fig. 6b). Similarly, out of a total 15 basic rocks, three rocks (AC-21A, AC-50, and AC-80 are characterized by $\leq 1 \times 10^{-6}$ m$^3$ kg$^{-1}$ and these rocks may be considered as intensively altered and the remaining 12 basic rocks are less altered (Fig. 6c).

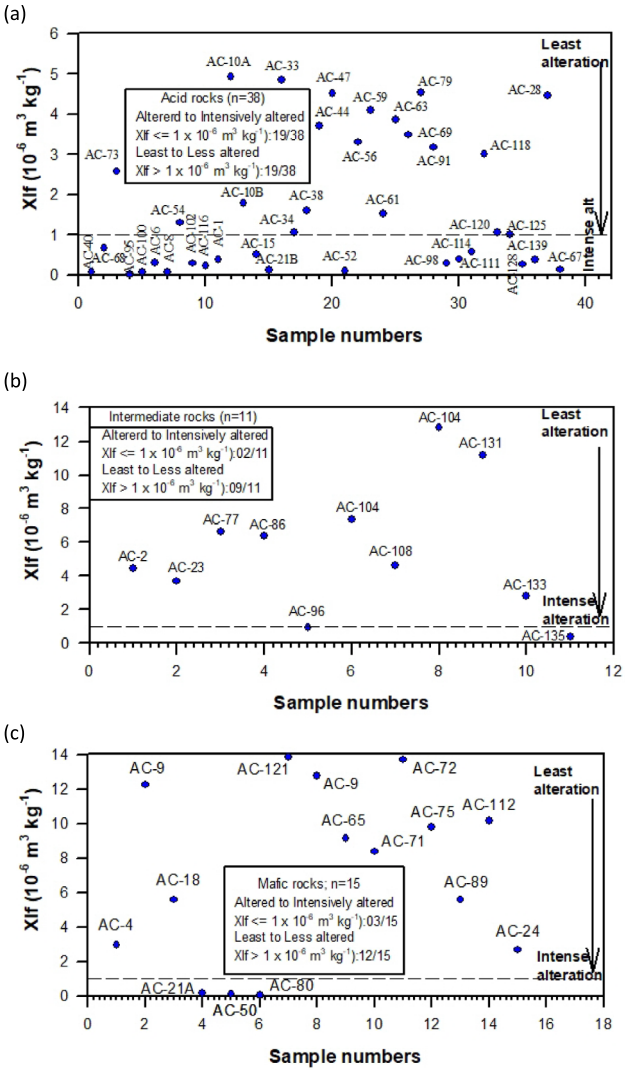


**Fig. 6** The binary diagrams of Sample Numbers versus $\chi lf \times 10^{-6}$ m$^3$ kg$^{-1}$ for acidic (**a**), intermediate (**b**) and for basic rocks (**c**)

The χlf values of the rock samples of the present work are higher than the average values reported for surface rhyolite (acid; $2.0 \times 10^{-6}$ m$^3$ kg$^{-1}$), trachyandesite (intermediate; $2.2 \times 10^{-6}$ m$^3$ kg$^{-1}$), and basalt (basic; $1.9 \times 10^{-6}$ m$^3$ kg$^{-1}$) from LHGF, a geothermal field located in the same Mexican Volcanic Belt, MVB. The χlf values of AGF are higher than those reported for the surface from LHGF. This indicates that the hydrothermal alteration conditions are more intensive at LHGF compared to those prevailing at AGF. This interpretation is supported by the fact that despite both AGF and LHGF being high-temperature systems, AGF is liquid dominant, whereas LHGF is vapor dominant. However, the surface rocks of AGF are characterized by much lower χlf values (higher intensity of alteration) than those compiled and reported by Hunt et al. (1995) for the fresh igneous rocks, fresh acid igneous rocks, and fresh basic igneous rocks, whose χlf values vary between 1 and $100 \times 10^{-6}$ m$^3$ kg$^{-1}$, 0.014 and $13 \times 10^{-6}$ m$^3$ kg$^{-1}$, and 0.2 and $44 \times 10^{-6}$ m$^3$ kg$^{-1}$, respectively. These results follow the known effects of hydrothermal alteration in reducing χlf values of fresh rocks (high χlf values) to altered rocks (low χlf values; Lapointe et al. 1986; Ledesert et al. 1999; Pandarinath et al. 2014; Nédélec et al. 2015).

### 4.3.1 *Percentage of frequency dependent susceptibility*

The percentage frequency-dependent susceptibility (χfd%) is a measure of the occurrence of very fine magnetic domains on the superparamagnetic (SP) to stable single domain (SSD). It represents the concentration and magnetic grain size and indicates the presence of ultrafine (diameter < 0.03 μm) superparamagnetic particles (SP), close to the SP/SD boundary (Thompson and Oldfield 1986; Jackson et al. 1993; Walden 1999). The literature reveals a relation between χfd% and magnetic grain size as follows: (1) χfd% values of < 3 and < 4 are dominated by frequency independent SSD and multy domain (MD) grains (Dearing et al. 1996, 1997); (2) the rocks with χfd% of < 2 are dominated by frequency-independent grains; χfd% of > 6 are dominated by frequency-dependent grains; and χfd% of 2–6 is an intermediate group consisting of a mixture of frequency-dependent and independent grains (Dearing et al. 1996, 1997); (3) the rock samples with χfd% < 2 and $\chi lf > 0.5 \times 10^{-6}$ m$^3$ kg$^{-1}$ samples are mostly pollution particles and igneous rocks containing SSD and MD ferrimagnetic grains (Dearing et al. 1996); (4) the proportions of SD (or SSD) grains are higher in the altered rocks than in the unaltered rocks (Dearing et al. 1996, 1997; Long et al. 2015; Nédélec et al. 2015); and (5) as a result of hydrothermal alteration, some of the primary MD grains of the rocks are dissolved and the crystallization of secondary SD grains takes place (Long et al. 2015; Nédélec et al. 2015). Hence, hydrothermal alteration is responsible for the dissolution of some of the primary MD magnetites associated with the crystallization of secondary SD grains (Dearing et al. 1996). Based on these observations it may be considered that the rock samples located in the zone defined by $\chi lf$ values of $< 0.5 \times 10^{-6}$ m$^3$ kg$^{-1}$ and χfd% values of 2–10 in the binary diagram χlf versus χfd% of Dearing et al. (1996) as altered rocks.

38 acid rock samples are plotted in the binary diagram χlf versus χfd% of Dearing et al. (1996). χlf and χfd% values of these acid rocks vary from 0.01 to $4.92 \times 10^{-6}$ m$^3$ kg$^{-1}$ and from 0% to 15.46%, respectively (Fig. 7a). The rocks in which the χlf values are $< 0.5 \times 10^{-6}$ m$^3$ kg$^{-1}$ and χfd% values are between 2 and 10 do not contain any SP grains, and SD and SSD grains dominate the magnetic mineral assemblage. The rocks with the higher proportions of SD and SSD grains are indicative of relatively more alteration

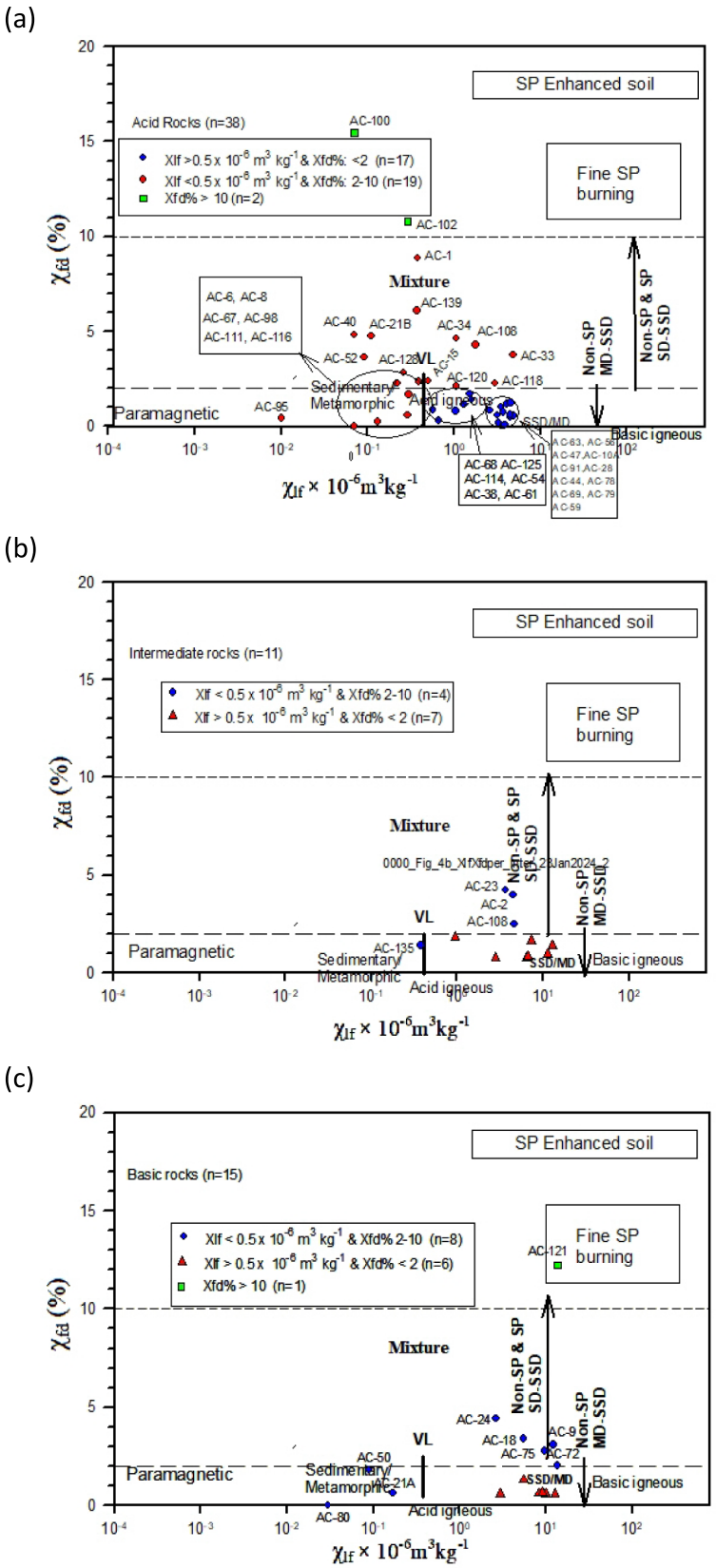


**Fig. 7** The binary diagram $\chi lf \times 10^{-6}$ m$^3$ kg$^{-1}$ versus $\chi fd\%$ for acidic (**a**), intermediate (**b**), and for basic rocks (**c**)

(Dearing et al. 1996). Based on this method 19 out of 38 acid rocks (AC-1, AC-6, AC-8, AC-10B, AC-15, AC-21B, AC-33, AC-34, AC-40, AC-52, AC-67, AC-95, AC-98, AC-111, AC-116, AC-118, AC-120, AC-128, AC-139; Fig. 7a), 4 out of 11 intermediate rocks (AC-2, AC-23, AC-108, and AC-135; Fig. 7b) and 8 out of 15 basic rocks (AC-9, AC-18, AC-21A, AC-24, AC-50, AC-72, AC-75, and AC-80; Fig. 7c) are identified as altered rocks.

## 5 Discussion

Plotting of rock samples in the binary diagram of the felsic component ($CaO + K_2O + Na_2O$) vs mafic component ($Fe_2O_3{}^T + MnO + MgO$) indicated that 15 out of a total of 38 acid rocks (Fig. 2a), five out of 11 intermediate rock samples (Fig. 2b) and eight out of the 15 basic rock samples (Fig. 2c) are least to less altered. Thus, 28 out of 64 rocks in total, are hydrothermally altered (Fig. 2a–c; Table S3). The two alteration indices CIA (Nesbitt and Young 1982) and WIP (Parker 1970) have provided consistent results, as both have indicated that 5 out of 11 intermediate rocks and 8 out of 15 basic rocks are altered. However, for acid rocks (n = 38), 17 are classified as altered by CIA (Fig. 3b), while 14 are indicated as altered by WIP (CIA, Fig. 3b; and WIP, |Fig. 3e). In the total 64 surface rocks, 30 and 27 rocks are classified as altered rocks by CIA and WIP indices, respectively. The χlf values obtained for acid rocks of the present study are (AGF; n = 38; 0.01 to $4.92 \times 10^{-6}$ $m^3$ $kg^{-1}$) within the range reported for acid igneous rocks (~$0.01–10 \times 10^{-6}$ $m^3$ $kg^{-1}$) by Dearing (1999). The classification of volcanic rocks based on χlf values is also supported by other techniques, such as the data for mineral composition. It indicates that 19 acid rocks have undergone intense silicification promoting the dissolution of primary minerals and precipitation of quartz and quartz polimorphs (Table S2). This interpretation is also supported by their mineral composition data consisting of feldspars, quartz, and quartz polymorphs in these 13 rocks, only quartz and quartz polymorphs in 5 rocks (AC-40, AC-52, AC-68, AC-95, AC-100) and the remaining one rock (AC-102) contained only clay minerals (dickite, and kaolinite). The mineral composition indicates that these 19 acid rocks have undergone an intense hydrothermal alteration (silicification) resulting in the complete dissolution of primary minerals and precipitation of quartz, and quartz polymorphs (Table S2).

These values are comparable to those obtained for the surface rhyolite rocks near the two drilled geothermal wells of the AGF (χlf values of $0–8.5 \times 10^{-6}$ $m^3$ $kg^{-1}$; Pandarinath 2020), and χlf values of $1.97 \times 10^{-6}$ $m^3$ $kg^{-1}$ for LHGF, Verma et al. 2018). An average χlf value of fresh andesite rocks varies between 0 and $61 \times 10^{-6}$ $m^3$ $kg^{-1}$ (Hunt et al. 1995). χlf values between 0.1 and $15.0 \times 10^{-6}$ $m^3$ $kg^{-1}$ for rhyolites and around $6\,500 \times 10^{-6}$ $m^3$ $kg^{-1}$ for andesites. The χlf values obtained for 38 acidic rocks vary between 0.01 and $4.92 \times 10^{-6}$ $m^3$ $kg^{-1}$ with 16 out of the 38 acidic rocks altered as they have low χlf values ($< 0.5 \times 10^{-6}$ $m^3$ $kg^{-1}$). From those 16, five samples show the highest hydrothermal alteration (lowest χlf values; $< 0.09 \times 10^{-6}$ $m^3$ $kg^{-1}$). Pandarinath et al. (2014, 2019) have successfully demonstrated the applicability and reliability of χlf in the identification of hydrothermally altered rocks and zones of hydrothermal alteration by applying them to the well rock cuttings of two geothermal wells of Los Azufres Geothermal Field of Mexico.

Based on the results of the magnetic properties of the intermediate rocks, it can be established that the samples with the greatest alteration (AC-2, AC-23, AC-96, AC-122, and AC-135) are those with the lowest concentration of χlf, and χfd%. Geochemical results show that there is an incomplete dissolution of ferromagnetic minerals and feldspars, while quartz and some polymorphs precipitate.

In the case of basic rocks, all samples have high concentrations of mafic elements, except for a sample AC-80. Seven samples show the highest concentrations of mafic and felsic minerals, while the remaining eight samples have a gradual decrease in the concentration of mafic minerals and a large loss of felsic minerals.

Furthermore, the basic rock samples with the greatest alteration according to χlf and χfd% (AC-80, AC-50, AC-9, AC-121, AC-18, AC-24, AC-4, and AC-21A) contain quartz polymorphs, halloysite, wheatleyite, hematite, and maghemite. However, three rock samples AC-21A, AC-50, and AC-80, are intensively altered, characterized by high CIA values (90.8–63.9), low WIP values (15.1–40.4), highest contents of sulfur (980–27000 ppm) and quartz, lowest content of feldspars, and the lowest values of χlf ($0.03–0.17 \times 10^{-6}$ $m^3$ $kg^{-1}$). However, three samples (AC-9, AC-24, and AC-121) have high CIA (75.6–96.1), low WIP (4.7–34.8), high LOI (10.3–18.8 wt%), and high S (40–90 wt%) but exhibit high values of the χlf ($2.7–13.7 \times 10^{-6}$ $m^3$ $kg^{-1}$), corresponding to fresh samples. Higher values of χlf for these rocks are explained by the presence of magnetic minerals. In fact, hematite and maghemite are identified by XRD and they are products of hydrothermal alteration of magnetite, both at high and low temperatures.

A comparison of results obtained by different methods applied in the identification of hydrothermal alteration and the average number of rocks identified as least to less altered and altered to intensively altered are presented in Table 1. Similarly, the alteration status of each rock for each method is reported in Table S3. The interrelation between some of the applied methods is evaluated by correlation coefficients (significant at $p$-value < 0.05). In the acid rocks, as following: (1) The strong negative correlation between CIA and

WIP values ($r = -0.9$) suggest the higher the CIA and the lower will be WIP values; the increase in CIA value indicate an increase in the intensity of alteration, whereas the decrease in the WIP values imply an increase in the intensity of alteration; (see the compiled data presented in the Table 1 of Pandarinath 2022); (2) the significant positive correlations between CIA and LOI ($r = 0.5$, Fig. 8b), and CIA and S ($r = 0.3$) infers that an increase in the intensity of alteration (increase in CIA) causes an increase in the LOI and S contents; (3) the positive correlation between LOI and S ($r = 0.6$) suggest that if LOI content of the rocks increases, the S content also increasers, and vice versa; and (4) the negative correlation between χlf and CIA ($r = -0.4$) and the positive correlation χlf and WIP ($r = 0.4$) deduces that the increase in the intensity of alteration (increase in CIA and decrease in WIP) effects an increase in the dissolution of Fe-minerals (magnetic minerals) and Fe-bearing minerals and precipitation of quartz and feldspars, finally resulting in to the lower χlf values.

The interrelation between some of the applied methods for intermediate and basic rocks reveals that: (1) as in the case of acid rocks, there is a strong negative correlation between CIA and WIP in intermediate rocks ($r = -0.9$) and in basic rocks ($r = -1.0$) suggesting that an increase in CIA value indicate an increase in the intensity of alteration, whereas the decrease in the WIP values imply an increase in the intensity of alteration; (2) there is a strong positive correlation between CIA and LOI ($r = 1.0$; Fig. 8b) in intermediate rocks and basic rocks ($r = 0.9$) infers that an increase in the intensity of alteration (increase in CIA) causes an increase in the LOI content in intermediate and basic rocks. There are no more significant correlations between the parameters in intermediate rocks, except one more significant correlation between χlf and S ($r = -0.5$) in basic rocks. This correlation between magnetic susceptibility (χlf) and S contents reveals that an increase in χlf causes a decrease in S content in basic rocks. As there is no direct relation between χlf and S, it may be considered that an increase in the intensity of alteration causes the dissolution of magnetic and/or Fe-bearing minerals resulting in a decrease in χlf values. An increase in the intensity of alteration may increase in S content.

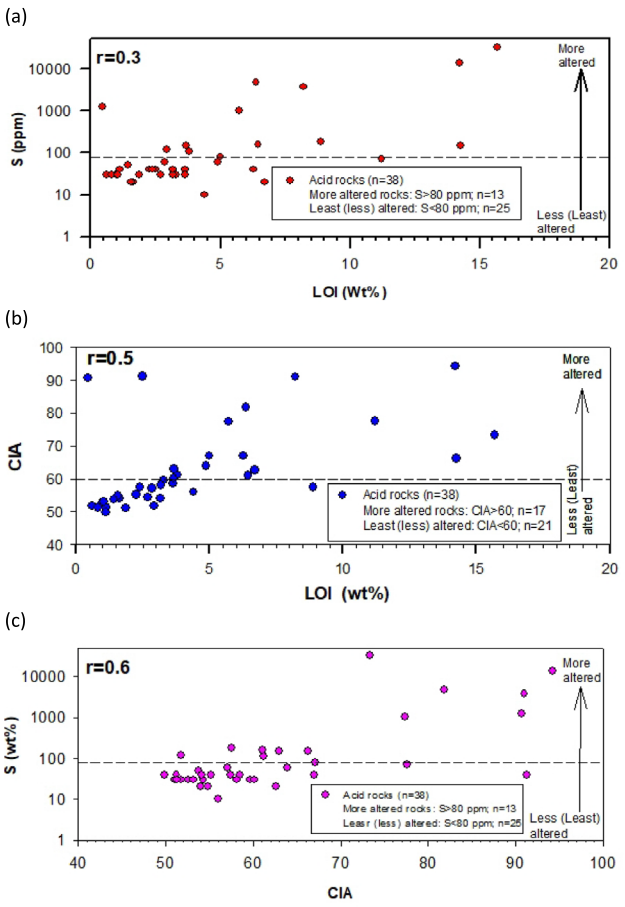


**Fig. 8** The binary diagrams of LOI versus S content (**a**), LOI versus CIA (**b**), and CIA versus S content (**c**) for each rock type

This shows that hydrothermal alteration of the rocks results in the dissolution of magnetic minerals and lower χlf values. An average χlf value of fresh andesite rocks reported in the range varies between 0 and $61 \times 10^{-6}$ m$^3$ kg$^{-1}$ (Hunt et al. 1995). They have also reported that the magnetic susceptibility of rhyolite, intermediate, and basic rocks varies between $0.1–15 \times 10^{-6}$ m$^3$ kg$^{-1}$, 65.0, and $0.084–61.0 \times 10^{-6}$ m$^3$ kg$^{-1}$, respectively. World average igneous rocks contain χlf of $1.0–100.0 \times 10^{-6}$ m$^3$ kg$^{-1}$, average acidic igneous rocks contain $0.014–31 \times 10^{-6}$ m$^3$ kg$^{-1}$, and average basic igneous rocks between 0.20 and $44 \times 10^{-6}$ m$^3$ kg$^{-1}$ (Torres-Alvarado et al. 2007). In the present study, χlf of the total 38 acid rocks varies between 0.01 and $4.92 \times 10^{-6}$ m$^3$ kg$^{-1}$ and is significantly lower than the χlf of rhyolite rocks ($0.1–15 \times 10^{-6}$ m$^3$ kg$^{-1}$) and average acidic igneous rocks ($0.014–31 \times 10^{-6}$ m$^3$ kg$^{-1}$) reported by Hunt et al. (1995).

Low χfd% values and/or higher proportions of SD (or young SSD) grains are characteristic of relatively more altered rocks. Nédélec et al. (2015) have reported that hydrothermal alteration of magnetite-bearing A-type granites has caused a decrease in magnetite contents, which in turn resulted in a lowering of the magnetic susceptibility of these rocks. They have also reported that the hydrothermal alteration is responsible for the dissolution of some of the primary MD magnetites and the crystallization of secondary SD grains, which has resulted in higher proportions of SD grains in the altered than in the unaltered rock samples. The binary diagram (χlf vs. χfd%) of Dearing (1996, 1999) is used to differentiate fresh and altered rocks (Fig. 7a–c). The rock samples plotted in the zone represented by χfd% values of 2–10 and $\chi lf < 0.5 \times 10^{-6}$ m$^3$ kg$^{-1}$ indicate that these rocks

do not contain SP grains, and SD and SSD grains dominate the magnetic mineral assemblage. The rocks with higher proportions of SD and SSD grains and with χfd% values of 2–10 and $\chi lf < 0.5 \times 10^{-6}$ $m^3$ $kg^{-1}$ are indicative of relatively more altered (Dearing 1999). 31 out of a total 64 rock samples of the present study are altered rocks (Fig. 7a–c). In the present study 19 out of 38 acid rocks (Fig. 7a), 4 out of the 11 intermediate rocks (Fig. 7b), and 8 out of 15 basic rocks (Fig. 7c) have been plotted in the zone with χlf values of $< 0.5 \times 10^{-6}$ $m^3$ $kg^{-1}$ and χfd% values of 2–10 (Fig. 7a–c). As this diagram has not yet been validated, we have not presented the localization of the hydrothermally altered surface rocks in Fig. 1. Both altered and less altered rocks are present on or near fault zones in AGF area (Fig. 1). We suggest that altered rocks relate to faults with a direct connection to the deep hydrothermal system, where thermal water and gases emanate to the surface, modifying the rocks. In the case of unaltered rocks near or on faults, we suggest that a self-sealing of these structures occurred as a consequence of mineral precipitation at depth, blocking the emanation of gases and thermal waters to the surface. Furthermore, this interpretation is also supported by the literature (Lopez-Hernandez and Castillo-Hernadez 1997; López-Hernández et al. 2009; Canet et al. 2010, 2015; Bólos et al. 2022). Notwithstanding, further application of these methods in other locations is needed to support better such conclusions.

## 6 Conclusions

The study on chemical, mineralogical, and rock magnetic parameters of the surface volcanic rocks of the Acoculco Geothermal Field (AGF) reveals that some of the existing chemical methods (chemical alteration indices, CIA and WIP; LOI; and S content) and newer methods (felsic and mafic components of major elements oxides, χlf and χfd%) in identification of hydrothermally altered rocks from the surface of AGF are equally effective in the identification of hydrothermally altered rocks from the surface of AGF. In these rocks, it is observed that χlf values of acid rocks < intermediate rocks < basic rocks, which shows the lithological influence on these parameters. At AGF, the most altered surface acid rocks are characterized by entirely quartz and its polymorphs, and clay minerals. The rock magnetic parameters χlf and χfd% are easy to measure, cost-effective, and have the potential to become reliable additional tools for future exploration studies. The present study, apart from providing the multi-parametric based alteration record for the surface region of AGF, also served in validating the application of the magnetic properties of rocks in the identification of the hydrothermally altered surface rocks, which can be useful during the initial stages of geothermal exploration.

**Acknowledgements** Rock magnetic instruments used in this work were procured with funding from CEMIE Geo project 207032 (Fondo de Sustentabilidad Energética de CONACyT-SENER, Government of Mexico). We would like to convey our thanks to: María Luisa Ramón García of IER-UNAM for her help with the XRD analyses of the rock samples; David Yáñez Dávila for his help in powdering the rock samples and also for preparing the modified Fig. 1 with the sample locations; Mirna Guevara García for her help in maintaining the laboratory. We are also thankful to all those who participated in the fieldwork in collecting the rock samples used in this work.

**Author contributions** AYGS: laboratory work, data generation, data analysis, and literature survey; KP: interpretation, writing, and overall supervision; ES: review and editing; EGP: fieldwork, sample collections, and review.

**Funding** Rock magnetic instruments used in this work are procured with the funding from CEMIE Geo project 207032 (Fondo de Sustentabilidad Energética de CONACyT-SENER, Government of Mexico). This project is completed, and at present, no funding is available for this project.

**Data availability** The data of the manuscript can be found in the Supplementary Tables and will be made available to the request by E-mails from the corresponding author (pk@ier.unam.mx).

**Declarations**

**Conflict of interest** The authors declare no conflict of interests.



## References

Anderson AT (1974) Chlorine, sulfur, and water in magmas and oceans. Geol Soc Am Bull 85:1485–1492

Arikawa Y (1987) Sulfur content of volcanic rocks in Japan. Bull Chem Soc Jpn 60:885–890

Avellán DR, Macías JL, Arce JL, Jiménez A, Saucedo-Girón R, Garduño-Monroy VH, Rangel E (2018) Eruptive chronology and tectonic context of the late Pleistocene Tres Vírgenes volcanic

complex, Baja California Sur (méxico). J Volcanol Geoth Res 360:100–125
Avellán DR, Macías JL, Layer PW, Cisneros G, Sánchez-Núñezç JM et al (2019) Geology of the late Pliocene – Pleistocene Acoculco caldera complex, eastern Trans-Mexican volcanic belt (México). J Maps 15(2):8–18. https://doi.org/10.1080/17445647.2018.1531075
Avellán DR, Macías JL, Layer PW, Sosa-Ceballos G, Gomez-Vasconcelos MG, Cisneros-Máximom G, Sánchez-Núnez JM, Martí J, García-Tenorio F, López-Loera H, Pola A (2020) Eruptive chronology of the Acoculco caldera complex–a resurgent caldera in the eastern Trans-Mexican volcanic belt (México). J South Am Earth Sci 98:402–412
Berger BR (1998) Hydrothermal alteration. Geochemistry. Encyclopedia of Earth science. Springer, Dordrecht
Bolós X, Del Angel V, Villanueva-Estrada RE, Sosa-Ceballo G, Boijseauneau-López M, Méndez MJL (2022) Surface hydrothermal activity controlled by the active structural system in the self-sealing geothermal field of Acoculco (Mexico). Geothermics 101:101237
Browne PRL (1978) Hydrothermal alteration in active geothermal fields. Annu Rev Earth Planet Sci 6:229–250
Browne PRL, Ellis AJ (1970) The Ohaki-broadlands hydrothermal area, New-Zealand: Mineralogy and related chemistry. Am J Sci 269:97–133
Canet C, Arana L, González-Partida E, Prol-Ledesma RM, Franco SI, Villanueva-Estrada RE, Camprubí A, Ramírez-Silva G, López-Hernández A (2010) A statistics based method for the short-wave infrared spectral analysis of altered rocks: An example from the Acoculco Caldera, Eastern Trans-Mexican volcanic belt. J Geochem Explor 105:1–10
Canet C, Hernández-Cruz B, Jiménez-Franc A, Pi T, Peláez B, Villanueva-Estrada RE, Alfonso P, González-Partida E, Salinas S (2015) Combining ammonium mapping and short-wave infrared (SWIR) reflectance spectroscopy to constrain a model of hydrothermal alteration for the Acoculco geothermal zone, Eastern Mexico. Geothermics 53:154–165
Dearing JA, Dann RJL, Hay K, Lees JA, Loveland PJ, Maher BA, O'Grady K (1996) Frequency-dependent susceptibility measurements of environmental materials. Geophys J Int 124:228–240
Dearing JA, Bird Dann JL, Benjamin SF (1997) Secondary ferrimagnetic minerals in Welsh soils: A comparison of mineral magnetic detection methods and implications for mineral formation. Geophys J Int 130:727–736
Dearing J (1999) Magnetic susceptibility. In: Walden J, Smith J, Oldfield F (Eds.), Environmental magnetism – A practical guide. Quaternary Research Association, London, Technical Guide, No. 6, pp 35–62
Franco A (2016) Subsurface geology and hydrothermal alteration of Cachaços-Lombadas sector, Ribeira Grande Geothermal Field. United Nations University Geothermal Training Programme, Sao Miguel Island, Azores, (UNUGTP) 2015 annual book (chapter 10), pp. 113–160
Geiss CE, Egli R, Zanne W (2008) Direct estimates of pedogenic magnetite as a tool to reconstruct past climates from buried soils. J Geophys Res 113:1–15
Gifkins C, Allen R, McPhie J (2005) Apparent welding textures in altered pumice-rich rocks. J Volcanol Geotherm Res 142:29–47
González-Partida E, Camprubí A, López-Hernández A, Santoyo E, Izquierdo-Montalvo G, Pandarinath K, Yáñez-Dávila D, González-Ruiz LE, González-Ruiz D, Díaz-Carreño E, Juárez-Hilarios E (2022) Distribution of hypogene alteration and fluid evolution in the Los Humeros geothermal field (Puebla, Mexico): multiple sourced fluids, interrelations, and processes in a superhot system. Appl Geochem 136:105159
Hatfield RG, Maher BA (2009) Holocene sediment dynamics in an upland temperate catchment: Climatic and land-use impacts in the English Lake district. Holocene 19:427–438
Hikov A (2002) Geochemistry of hydrothermally altered rocks in K.lisoura occurrence, Sofia District. Geol Balc 32:89–92
Hoffmann V, Knab M, Appel E (1999) Magnetic susceptibility mapping of roadside pollution. J Geochem Explor 66:313–326
Hunt PC, Moskowitz BM, Banerjee SK (1995) Magnetic properties of rocks and minerals. In: Rock physics and phase relations, a handbook of physical constants. American Geophysical Union (AGU) Reference Shelf 3:189–204
Jackson MP, Rochette G, Fillion S, Banerjee J, Marvin (1993) Rock magnetism of remagnetized Paleozoic carbonates: Low-temperature behavior and susceptibility characteristics. J Geophys Res 98:6217–6225
Jayawardena U, Izawa E (1994) Application of present indices of chemical weathering for Precambrian metamorphic rocks in Sri Lanka. Bull Int Assoc Eng Geol 49:55–61
Johnson WM, Maxwell JA (1981) Rock and mineral analysis, 2nd edn. Wiley-Interscience, New York, p 489
Lagat J (2009) Hydrothermal alteration mineralogy in geothermal fields with the case example from Olkaria Domes geothermal fields, Kenya. In: Presentation-short course IV on exploration for geothermal resources. UNU-GTP, KenGen and GSC, Kenya, p 24
Lapointe P, Morris WA, Harding KL (1986) Interpretation of magnetic susceptibility: A new approach to geophysical evaluation of the degree of rock alteration. Can J Earth Sci 23:393–401
Larrasoaña JC, Roberts AP, Musgrave RJ, Gràcia E, Piñero P, Vega M, Martínez-Ruiz F (2007) Diagenetic formation of greigite and pyrrhotite in gas hydrate marine sedimentary systems. Earth Planet Sci Lett 261:350–366
Le Bas MJ, Le Maitre RW, Streckeisen A, Zanettin B (1986) A chemical classification of volcanic rocks based on the total alkali-silica diagram. J Petrol 27:745–750
Lechler PJ, Desilets MO (1987) A review of the use of loss on ignition as a measurement of total volatiles in whole-rock analysis. Chem Geol 63:341–344
Ledésert B, Berger G, Meunier A, Genter A, Bouchet A (1999) Diagenetic-type reactions related to hydrothermal alteration in the Soultzsous-Forêts granite. Eur J Mineral 11:731–741
Long X, Ji J, Balsam W, Barrón V, Torrent J (2015) Grain growth and transformation of pedogenic magnetic particles in red Ferralsols. Geophys Res Lett 42:5762–5770
López-Hernández A, Castillo-Hernández D (1997) Exploratory drilling at Acoculco, Puebla, Mexico: A hydrothermal system with only nonthermal manifestations. Geotherm Resour Counc Trans 21:429–433
López-Hernández A, García-Estrada G, Aguirre-Díaz G, González-Partida E, Palma Guzmán H, Quijano-León JL (2009) Hydrothermal activity in the Tulancingo Acoculco Caldera complex, central Mexico: Exploratory studies. Geothermics 38:279–293
MacKenzie DJ, Craw D (2007) Contrasting hydrothermal alteration mineralogy and geochemistry in the auriferous rise & shine shear zone, Otago, New Zealand. New Zeal J Geol Geophys 50:67–79
Mahe BA, Thompson R, Zhou LP (1994) Spatial and temporal reconstructions of changes in the Asian palaeomonsoon: A new mineral magnetic approach. Earth Planet Sci Lett 125:461
Maher BA, Taylor RM (1988) Formation of ultrafine-grained magnetite in soils. Nature 336:368–370
Maher BA, Hu M, Roberts HM, Wintle AG (2002) Holocene loess accumulation and soil development at the western edge of the Chinese loess plateau: Implications for magnetic proxies of paleorainfall. Quat Sci Rev 22:445–451
Matsuno S, Uno M, Okamoto T, Suchiya N (2022) Machine-learning techniques for quantifying the protolith composition and mass

transfer history of metabasalt. Sci Rep Nat Portf 12:1385. https://doi.org/10.1038/s41598-022-05109-x
McLennan SM (1993) Weathering and global denudation. J Geol 101:295–303
Moore JG, Fabbi BP (1971) An estimate of the juvenile sulfur content of basalt. Contr Mineral Petrol 33:118–127
Naldrett AJ, Goodwin AM, Fisher TL, Ridler RH (1978) The sulfur content of Archean volcanic rocks and a comparison with ocean floor basalt. Can J Earth Sci 15:715–728
Nédélec A, Trindade R, Peschler A, Archanjo C, Macouina M, Poitrasson F, Bouchez JL (2015) Hydrothermally induced changes in mineralogy and magnetic properties of oxidized A-type granites. Lithos 212–215:145–157
Nesbitt HW, Young GM (1982) Early Proterozoic climates and plate motions inferred from major element chemistry of lutites. Nature 299:715–717
Nesbitt HW, Young GM (1984) Prediction of some weathering trends of Plutonic and volcanic rocks based on thermodynamic and kinetic considerations. Geochim Cosmochim Acta 48:1523–1534
Oldfield F (1991) Environmental magnetism—A personal perspective. Quat Sci Rev 10:73–78
Oliva-Urcia O, Kontny A, Vahle C, Schleicher AM (2011) Modification of the magnetic mineralogy in basalts due to fluid–rock interactions in a high-temperature geothermal system (Krafla, Iceland). Geophycs J Int 186:155–174. https://doi.org/10.1111/j.1365-246X.2011.05029
Pandarinath K (2022) Application potential of chemical weathering indices in the identification of hydrothermally altered surface volcanic rocks from geothermal fields. Geosci J 26:415–442
Pandarinath K, Shankar R, Alvarado IST, Warrier AK (2014) Magnetic susceptibility of volcanic rocks in geothermal areas: Application potential in geothermal exploration studies for identification of rocks and zones of hydrothermal alteration. Arab J Geosci 7:2851–2860
Pandarinath K, Shankar R, Santoyo E, Shwetha S, García-Soto AY, Gonzalez-Partida E (2019) A rock magnetic fingerprint of hydrothermal alteration in volcanic rocks - an example from the Los Azufres geothermal field, Mexico. J South Am Earth Sci 91:260–271
Pandarinath K, García-Soto AY, Santoyo E, Guevara M, Gonzalez-Partida E (2020) Mineralogical and geochemical changes due to hydrothermal alteration of the volcanic rocks at Acoculco geothermal system. Mexico Geol J 55:6508–6526
Pandarinath K, Rivas-Hernández JL, Arriaga-Fuentes JA, Yáñez-Dávila D, González-Partida E, Santoyo E (2023) Hydrothermal alteration of surficial rocks at Los Humeros geothermal field, Mexico: A magnetic susceptibility approach. Arab J Geosci 16:259
Parker A (1970) An index of weathering for silicate rocks. Geol Mag 107:501–504
Pereira ML, Matias D, Viveiros F, Moreno L, Silva C, Zanon V, Uchôa J (2022) The contribution of hydrothermal mineral alteration analysis and gas geothermometry for understanding high-temperature geothermal fields– the case of Ribeira Grande geothermal field, Azores. Geothermics 105:102519. https://doi.org/10.1016/j.geothermics.2022.102519
Pirajno F (2009) Hydrothermal processes and wall rock alteration. Hydrothermal processes and mineral systems. Springer, Dordrecht
Riveros K, Veloso E, Campos E, Menzis A, Véliz W (2014) Magnetic properties related to hydrothermal alteration processes at the Escondida porphyry copper deposit, northern Chile. Miner. Deposita 49:693–703
Roberts AP, Turner GM (1993) Diagenetic formation of ferrimagnetic iron sulphide minerals in rapidly deposited marine sediments, South Island, New Zealand. Earth Planet Sci Lett 115:257–273. https://doi.org/10.1016/0012-821X(93)90226-Y
Rudnick RL, Gao S (2003). Treatise on geochemistry. In: RL Rudnick, HD Holland, KK Turekian, Elsevier, Amsterdam, pp 1–64
Sánchez-Córdova MM, Canet C, Rodríguez-Díaz A, González-Partida E, Linares-López C (2020) Water-rock interactions in the Acoculco geothermal system, eastern Mexico: Insights from paragenesis and elemental mass-balance. Geochemistry 80:125527
Sosa-Ceballos G, Macías JL, Avellán DR, Salazar-Hermenegildo N, Boijseauneau-López ME, Pérez-Orozco JD (2018) The Acoculco Caldera Complex magmas: genesis, evolution and relation with the Acoculco geothermal system. J Volcanol Geotherm Res 358:288–306
Stefánsson A, Kleine BI (2017) Hydrothermal alteration. In: White W (ed) Encyclopedia of geochemistry. Encyclopedia of Earth sciences series. Springer, Cham
Suoeka T, Lee IK, Huramatsu M, Imamura S (1985) Geomechanical properties and engineering classification for decomposed granite soils in Kaduna district, Nigeria. In: Proceedings 1st International Conference on Geomechanics in Tropical Lateritic and Saprolitic Soils, Brasilia, Publ 1, pp 175–186
Takahashi F, Shimaok T (2012) The weathering of municipal solid waste incineration bottom ash evaluated by some weathering indices for natural rock. Waste Manag 32:2294–2305
Thompson R, Oldfield F (1986) Environmental magnetism. Allen & Unwin, London
Torres-Alvarado IS, Pandarinath K, Verma SP, Dulski P (2007) Mineralogical and geochemical effects due to hydrothermal alteration in the Los Azufres geothermal field, Mexico. Rev Mex De Cienc Geol 24:15–24
Turekian KK, Wedepohl KH (1961) Distribution of the elements in some major units of the Earth's crust. Geol Soc Am Bull 72:175–192
Verma SP (2001) Geochemical evidence for a lithospheric source for magmas from Acoculco Caldera, Eastern Mexican volcanic belt. Int Geol Rev 4:31–51
Verma SP, Rivera-Gómez MA, Díaz-González L, Pandarinath K, Amezcua-Valdez A, Rosales-Rivera M, Verma SK, Quiroz-Ruiz A, Armstrong-Altrin JS (2017) Multidimensional classification of magma types for altered igneous rocks and application to their Tectonomagmatic discrimination and igneous provenance of siliciclastic sediments. Lithos 278–281:321–330
Verma SP, Pandarinath K, Bhutani R, Dash JK (2018) Mineralogical, chemical, and Sr-Nd isotopic effects of hydrothermal alteration of near-surface rhyolite in the Los Azufres geothermal field, Mexico. Lithos 322:347–361
Viggiano-Guerra JC, Flores-Armenta M, Ramírez-Silva GR (2011) Evolución del sistema geotérmico de Acoculco, Puebla, México: un estudio con base en estudios petrográficos del pozo EAC-2 y en otras consideraciones. Geotermia Revista Mexicana De Geoenergía 24:14–24
Walden J (1999) Remanence measurements. In: Walden J, Oldfield F, Smith J (Eds.) Environmental magnetism: A practical guide. Quaternary Research Association, London, Technical Guide, no. 6, pp 63–88
Walling DE, Peart MR, Oldfield F, Thompson R (1979) Suspended sediment sources identified by magnetic measurements. Nature 281:110–113
Weyd L, Lucci F, Lacinska A et al (2022) The impact of hydrothermal alteration on the physiochemical characteristics of reservoir rocks: The case of the Los Humeros geothermal field (Mexico). Geotherm Energy 10:20. https://doi.org/10.1186/s40517-022-00231-5